Geofísica Internacional 47 (4), 355-369 (2008)

An exploratory study for rapid estimation of critical source parameters of great subduction-zone earthquakes in Mexico

S. K. Singh[1]*, X. Pérez-Campos[1], A. Iglesias[1] and J. F. Pacheco[1]
[1]*Instituto de Geofísica, Universidad Nacional Autónoma de México, Mexico City, Mexico*

Received: March 5, 2008; accepted: August 28, 2008

Resumen

Para una estimación oportuna del potencial de daño y tsunami asociado a los grandes temblores de subducción en México, resulta crítica la determinación rápida y confiable de parámetros sismológicos como lo son la magnitud de momento (M_w), la energía sísmica radiada (E_s) y la localización y el tamaño de la ruptura. Para alcanzar este objetivo, la red sismológica de banda ancha mexicana necesita ser complementada con estaciones GPS permanentes localizadas a lo largo de la costa del Pacífico mexicano espaciadas, por lo menos, cada 65 km. Los datos de esta red GPS requieren ser transmitidos a una estación central y procesados en tiempo real para monitorear la posición de las estaciones. Asumiendo que lo anterior estuviera implementado, en este trabajo desarrollamos una metodología para la estimación rápida de parámetros críticos de la fuente sísmica y demostramos su viabilidad aplicándola al análisis del sismo de Colima-Jalisco de 1995 (M_w=8.0) y de Sumatra-Andamán de 2004 (M_w=9.0-9.3). Para este par de temblores, la metodología propuesta arrojó valores de M_w y E_s que son muy similares a los reportados anteriormente, obtenidos a partir de análisis detallados. En el caso del sismo de Colima-Jalisco la localización estimada y el tamaño del área de ruptura están de acuerdo con los valores que se pueden inferir a partir de las localizaciones de las réplicas. Actualmente existen 13 estaciones GPS permanentes a lo largo de la costa del Pacífico mexicano con un espaciamiento promedio de ~200 km, las cuales operan de manera autónoma. Es urgente incrementar este número de estaciones a ≥28 (logrando un espaciamiento de ≤65 km), así como transmitir los datos y determinar la posición de las estaciones en tiempo real (preferiblemente cada segundo).

Palabras clave: Alerta de tsunami, sismología de tiempo real, grandes temblores mexicanos.

Abstract

The rapid and reliable estimation of moment magnitude M_w, location, and size of rupture area, and radiated energy E_s of great Mexican subduction zone earthquakes is critical for a quick assessment of tsunami and/or damage potential of the event and for issuing an early tsunami alert. To accomplish this goal, the Mexican broadband seismic network needs to be supplemented by permanent GPS stations along the Pacific coast, spaced about 65 km apart or less. The data from the GPS network must be transmitted to a central location and processed in near-real time to track the position of the stations. Assuming that this can be implemented, we develop a procedure for near-real time estimation of the critical source parameters. We demonstrate the viability of the procedure by processing near-source GPS data and regional seismograms for the earthquakes of Colima-Jalisco in 1995 (M_w=8.0) and Sumatra-Andaman in 2004 (M_w=9.0-9.3). The procedure yields estimates of M_w and E_s in excellent agreement with those reported from earlier solutions. In the case of the Colima-Jalisco earthquake, the estimated location and size of rupture area agree with that mapped from aftershock locations. Presently, there are 13 permanent GPS stations along the Pacific coast of Mexico with an average spacing of ~200 km which operate in an autonomous mode. It is urgent to increase the number of stations to ≥28 thus decreasing the spacing of stations to ≤65 km. Data must be transmitted in near-real time to a central station to track the position of the stations, preferably every second.

Key words: Tsunami alert, real time seismology, large Mexican earthquakes.

Introduction

Rapid estimation of critical source parameters of great ($M_w \geq 8.0$) subduction-zone earthquakes of Mexico is of importance to civil protection authorities in organizing post-seismic recovery. These parameters may provide a first glimpse at possible damage and casualties. They are also useful for early tsunami warning, a topic of general concern after the tsunami caused by the 26 December, 2004 Sumatra-Andaman earthquakes that killed about 200,000 people.

In the last century, several earthquakes have generated moderate, local tsunamis along the Pacific coast of Mexico, notably the Colima-Jalisco earthquakes of 3, 18, and 22 June, 1932, M=8.2, 7.6, 7.0, respectively; the Michoacan earthquake of 19 September, 1985, M_w=8.0; and the Colima-Jalisco earthquake of 9 October, 1995, M_w=8.0 (Farreras, 1997). There is also evidence of much larger tsunamis along the Mexican coast. For example, Suárez and Albini (2008) and Núñez-Cornu and Ortiz (2008), based on historical documents, suggest that the earthquake of 28 March, 1787 may have caused the largest

tsunami in Mexico since 1700. The earthquake probably ruptured a 400 km-long segment (M~8.4) along the coast of Oaxaca (Suárez and Albini, 2008). Early warning may not be useful to populations in the near-source region of Mexico unless it can be issued in less than 10 minutes or so. This is because the peak in the tsunami height may reach the coast about 10-15 minutes after the origin time of the earthquake (M. Ortiz, personal communication, 2007). Such a warning may, however, be quite useful for more distant coastal areas.

Rapid assessment of tsunami and/or damage potential of a great earthquake requires near-real time estimation of (1) the moment magnitude (M_w), (2) the location and the size of the rupture area, and (3) the radiated seismic energy (Es). An earthquake of great magnitude whose rupture area partly lies below the continent has relatively enhanced high-frequency radiation and will probably generate severe ground motions, causing damage to engineering structures and loss of life. On the other hand, when the rupture area lies offshore and the high-frequency radiation is relatively depleted, the earthquake may not produce large, destructive ground motions but may have a higher tsunamigenic potential. The challenge is to estimate these parameters rapidly. In this paper, we propose and partly validate a strategy for quick and reliable estimation of the parameters mentioned above. Finally, we discuss the steps needed for its routine implementation in Mexico.

Estimation of *Mw*, and the location and size of the rupture area

For great earthquakes, the desirable magnitude to be estimated is the moment magnitude, M_w, which is based on very long-period seismic waves and/or coseismic static deformation. Unlike magnitudes computed from amplitudes of shorter-period waves, M_w does not saturate. Regional broadband seismograms from the Mexican seismic network, alone, may not be sufficient to estimate M_w as these records may get clipped during great events. Even if the seismograms are on scale, very long-period waves may not be well developed at regional distances to permit reliable estimation of the seismic moment and, hence, of M_w of great earthquakes. For the Sumatra-Andaman earthquake, free-oscillation data at periods of about 1 hour were required to obtain a reliable estimate of M_w (Stein and Okal, 2005; Park *et al*., 2005; Lay *et al*., 2005). This estimate was later confirmed from modeling of static displacements observed in the near- and far-field (e.g., Banerjee *et al*., 2005; Vigny *et al*., 2005).

As broadband seismograms are not sufficient to determine M_w of great earthquakes in Mexico, we must complement them with data on static displacements. Double integration of accelerograms might also provide the desired static displacement field: for example, the near-field accelerogram recorded at Caleta de Campos (CALE) during the Michoacan earthquake of 19 September, 1985, M_w=8.0, when integrated (Fig. 1), indicated an uplift of the coast by 1 m (Anderson *et al*., 1986). This was independently confirmed from data on mortality of intertidal organisms (Bodin and Klinger, 1986). However, double integration of accelerograms is often unreliable because of baseline offsets in the acceleration time history, hysteresis of the accelerometer, and possible tilt and rotation of the site (e.g., Iwan *et al*., 1985; Boore, 2001; Clinton, 2004; Emore *et al*., 2007). As Fig. 1 shows, the static displacement at CALE for the Michoacan earthquake was not obtained by simple double integration of the accelerogram but involved some subjective judgment. It follows that permanent GPS stations, whose positions can be tracked in near real time, may be required for rapid mapping of static displacement field caused by great earthquakes.

Fig. 2 shows theoretical surface displacements in the near field caused by shallow dipping, thrust earthquakes of M_w=8.0 and 8.4 buried in a half space. The calculations are based on Okada's model (1992). For both earthquakes, the fault is approximated by a rectangle of width, W, of 80 km and dip, δ, of 15^0. The rake, λ, is taken as 90^0. The deep edge of the fault is at a depth d of 25 km. Numerous studies on seismicity, and on large earthquakes and their aftershocks show that these parameters are reasonable for earthquakes with M_w>7.8 along the Mexican subduction zone, from Jalisco to Tehuantepec (see, e.g., Chael and Stewart, 1982; Singh *et al*., 1985; Singh and Mortera, 1992; Suárez *et al*., 1990; Pacheco and Singh, 2008). The fault parameters used in generating Fig. 2 are listed in Table 1.

Table 1

Magnitude	M_w=8.0	M_w=8.4
W *	80 km	80 km
L #	126 km	320 km
M_0 +	1.26x10^{21} Nm	5.01x10^{21} Nm
D $	310 cm	490 cm

*Width, W, of the fault fixed based on studies of Mexican subduction zone earthquakes

#Length, L, computed from the relation $Mw = log A + 4$, where A is the rupture area in km^2

+Seismic moment, M_0, obtained from log M_0= 1.5 M_w + 9.1

$Average slip, D, computed from $M_0 = \mu LWD$, where μ is the rigidity, taken here as 5x10^4 MPa

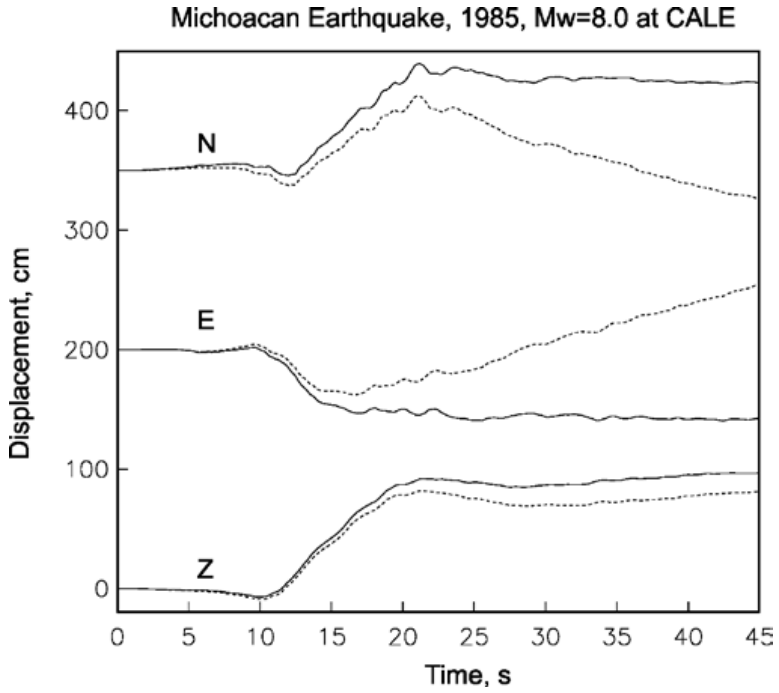

Fig. 1. Static displacement at CALE caused by the Michoacan earthquake of 1985. The station was located on the coast in the epicentral region of the earthquake. Continuous curve: from double integration of accelerogram but involving subjective baseline corrections; dashed curve: direct double integration of accelerogram after baseline correction using prevent data.

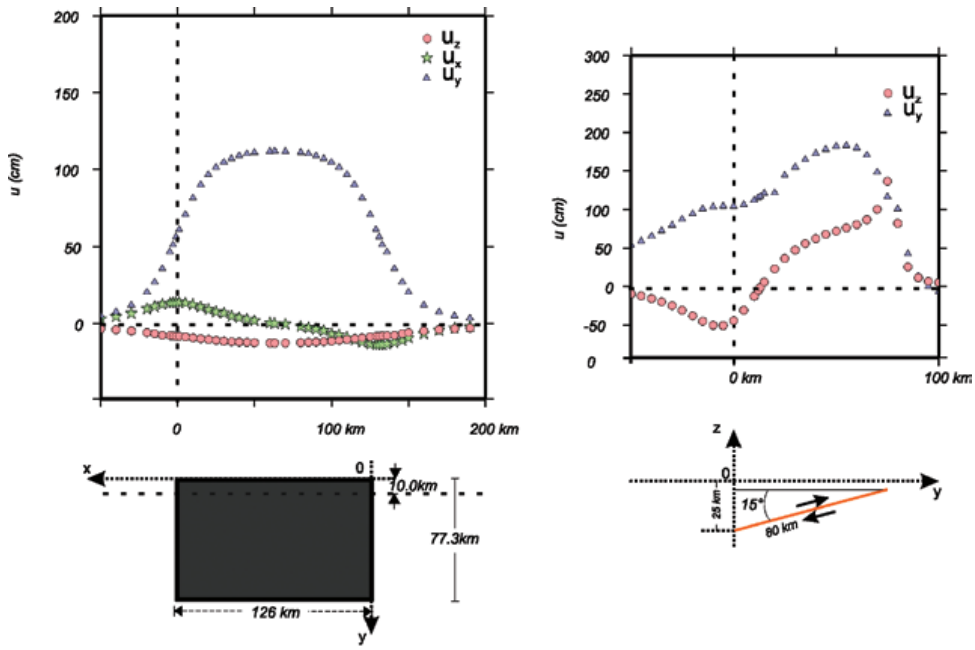

Fig. 2. Static displacement field caused by an earthquake of M_w=8 (above) and 8.4 (below), calculated from Okada's (1992) model. In both case, the fault is 80 km wide with its deep edge at y=0 and z=-25 km. (Left) Profile along the fault with y=10 km, and z=0. U_z (red circles): vertical displacement, U_x (green stars): horizontal displacement along the length of the fault, U_y (blue triangles): horizontal displacement along the width of the fault. (Right) Profile along the width of the fault; x=L/2 (L=126 km for M_w=8.0 and 320 km for M_w=8.4) and z=0. In this case, because of symmetry, U_y= 0. The model parameters are given in Table 1.

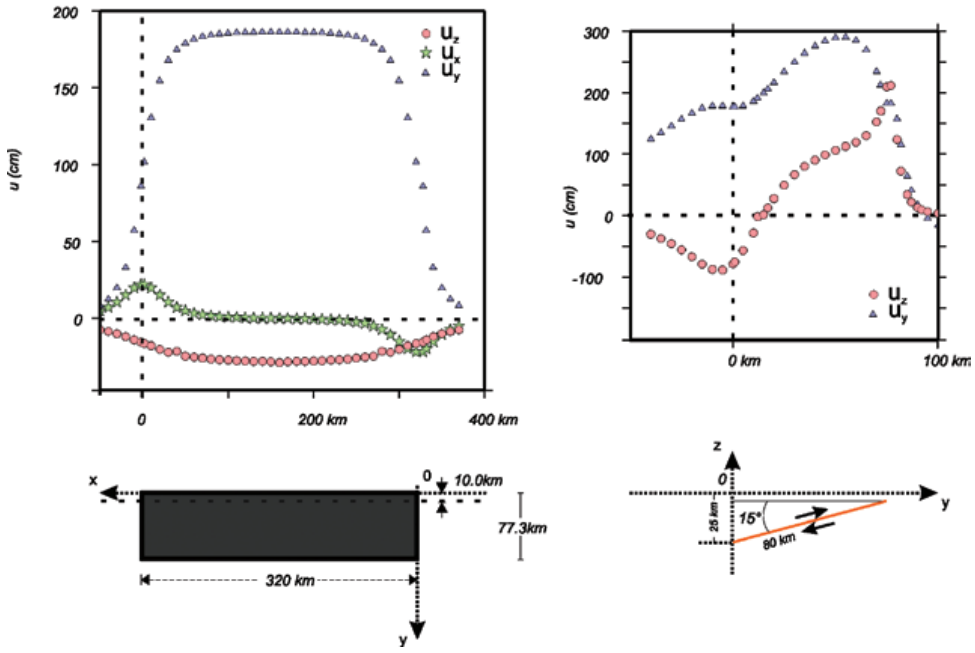

Fig. 2. (Continue)

The coordinate system used in the computation is the same as in Okada (1992). From frames on the right of Fig. 2 we note that: (1) the hinge line for vertical displacement, U_z, is at a distance of ~13 km toward the trench from the projection of the deepest part of the fault. With respect to the hinge line, U_z is negative towards the continent and positive towards the trench. (2) While magnitude and polarity of U_z are very sensitive to the position of observation point with respect to the hinge line, the horizontal displacement in the direction perpendicular to the strike of the fault (U_y, blue triangles) is much less so. (3) U_y falls off quickly beyond the edge of the fault.

These properties may be used to delimit the rupture areas of great earthquakes from observed static displacements along the Pacific coast of Mexico. For example, if *Uz* is negative along the coast (subsidence), the horizontal projection of the edge of the fault can be no further inland than 13 km from the coast. If, however, *Uz* is positive (uplift), then the fault projection must be more than 13 km inland. Consider the Michoacán earthquake of 19 September 1985 (M_w = 8.0). The earthquake caused an uplift of the coast by 1 m (Fig. 1). In this case, we would expect the rupture to extend more than 13 km inland. In fact, an aftershock study indicated that nearly half the rupture area was below the continent (UNAM Seismology Group, 1986). For this reason, only about half the rupture area would have been involved in the uplift of the ocean floor and in tsunami generation. In fact, the earthquake caused only a minor, local tsunami (Farreras, 1997).

The length of the fault can be roughly estimated from the amplitude of horizontal displacement vectors, since their amplitudes decay rapidly beyond the edge of the fault. Once the approximate dimension of the fault is known, the static horizontal displacements can be used to estimate M_0, and, hence, M_w of the earthquake. As we discuss later, a relatively dense array of GPS stations along the Pacific coast of Mexico will be required for reliable estimation of M_w.

We recall that the trench from Puerto Vallarta to Puerto Angel is ~80 km offshore. As *W* of $M_w \geq 7.6$ earthquakes is ~80 km, the horizontal projection of the deepest part of the rupture lies only slightly inland or offshore. As discussed above, in this case the location and size of the rupture can be estimated from static displacements observed on the coast. This may not be so for the subduction segment between Tehuantepec and Tapachula since the trench here is ~150 km offshore. In this case, it will be difficult to find the location and the size of the rupture from coastal static field data without careful analysis.

Radiated Energy

A large magnitude earthquake with a location near the trench of a subduction zone is potentially a tsunamigenic event. Such events may also be deficient in high-frequency radiation and, hence, give rise to relatively low accelerations on land. Tsunami earthquakes which, by definition, generate disproportionately large tsunamis in relation to their surface-wave magnitudes (Kanamori, 1972), are deficient in high-frequency radiation. Such events are characterized by large (M_s-M_w) and (m_b-M_w) disparity (Kanamori and Kikuchi, 1993; Kanamori, 2006), and anomalously low value of E_s/M_0 (Newman and Okal, 1998; Ammon *et al*., 2006), where M_s and m_b are surface-wave and short-period body-wave magnitudes, respectively. Clearly, a rapid estimation of E_s is important for understanding the nature of the source and detecting tsunami potential and/or damage potential of the earthquake. In fact, for early tsunami warning, the Pacific Tsunami Warning Center (PTWC) now calculates both long-period magnitude and E_s/M_0 in near-real time (Weinstein and Okal, 2005). The radiated energy at PTWC is estimated from the integration of velocity-squared P wave spectra at teleseismic distances following the method of Boatwright and Choy (1986).

For near-real time estimates of E_s of large Mexican earthquakes, we propose to use broadband records at regional distances. E_s can be estimated from integration of velocity-squared spectra of the S-wave group after applying corrections for anelastic attenuation and site effects (Singh and Ordaz, 1994; Pérez-Campos *et al*., 2003). E_s can also be estimated using the empirical Green's function (EGF) technique. This method has the advantage that it does not require corrections for attenuation and local site effects. Recordings of a smaller earthquake from the same region where a great earthquake has just occurred can be used as EGF. The location and focal mechanism of the EGF and the large, target event should be similar. However, a study by Venkataraman *et al*. (2002) suggests that the estimates are robust with respect to moderate difference in the focal mechanisms of the mainshock and the EGF. The magnitude of the target event should be at least 2 units greater than that of the EGF. Assuming point-source, far-field approximation to be valid, E_s can be written as (Vassiliou and Kanamori, 1982):

$$E_s = \frac{4\pi}{5\rho\beta^5} \int_0^\infty f^2 \dot{M}_0(f)\, df, \tag{1a}$$

where $\dot{M}_0(f)$ is the moment rate spectrum, ρ is the density and β is the shear-wave velocity in the source region. Let f_c be the corner frequency of the earthquake. At frequencies $f << f_c$, $\dot{M}_0(f) = M_0$, so that E_s in the frequency range of 0 to f_l, where $f_l << f_c$, is given by

$$E_s = \left(4\pi / 5\rho\beta^5\right) M_0^2 \left(f_l^3 / 3\right). \tag{1b}$$

For a Brune ω^2-source model (Brune, 1970)

$$\dot{M}_0(f) = \frac{M_0}{1+\left[\frac{f}{f_c}\right]^2},$$

so that for $f >> f_c$, $\dot{M}_0(f) \rightarrow M_0(f_c/f)^2$. In this case, E_s in the frequency band of f_u to ∞, where $f_u >> f_c$, is given by

$$E_s = \left(4\pi / 5\rho\beta^5\right) \dot{M}_0^2\left(f_u\right) f_u^3 . \tag{1c}$$

The following steps would be required for a rapid estimation of E_s of a great earthquake using the EGF technique:

(1) Locate the earthquake and determine its focal mechanism from regional moment tensor inversion.

(2) From computer archives containing recordings of moderate earthquakes with known location, M_0, corner frequency, and focal mechanism, retrieve the event whose location and mechanism is similar to that of the large earthquake.

(3) Compute spectral ratio of S-wave group of the large earthquake to the EGF event at each station.

(4) Multiply the ratios by the seismic moment of the EGF to obtain the median $\dot{M}_0(f)$.

(5) Use equations (1a) to (1c) to estimate E_s. The choice of the upper limit of integration, f_u, is critical since the corner frequency of the EGF affects $\dot{M}_0(f)$ (e.g., Iglesias and Singh, 2007). If M_w of the EGF is less than or equal to 6, then the upper limit of integration could be set to 0.2 Hz. The contribution to E_s from $f > 0.2$ Hz can be estimated assuming an ω^2 source model, using equation (1c).

An important factor in tsunami generation may be the depth of the source. If so, then rapid and reliable depth estimation would be helpful in early tsunami alert. Shapiro *et al*. (1998) report that the ratio of total to high-frequency energy, E_r, is a useful parameter in depth discrimination. These authors show that E_r of earthquakes along the Pacific coast of Mexico, recorded on a broadband seismograph at CUIG, a station in the UNAM campus in Mexico City ($3° \le \Delta \le 5°$), is sensitive to the depth of the event: shallower, near-trench events have larger E_r values than deeper ones (see also Iglesias *et al*., 2003). They suggest that earthquakes with large M_w and large E_r would have high tsunami potential. Such events also give rise to, relatively, lower accelerations (Iglesias *et al*., 2003).

The dependence of E_r on depth arises from the fact that seismograms of shallower events at regional distance are enhanced at longer periods as compared to the deeper

ones. In fact, slowness of the source would cause an effect on seismograms similar to the shallowness of the event. Since E_r is a ratio, the effect of focal mechanism is cancelled out. If path and distance from different events to a given station are roughly the same (thus requiring a minor correction to normalize the data to a common distance), then it should be possible to compare E_r values of different earthquakes in a meaningful manner. For this reason, E_r seems a useful parameter to compliment M_w, location of the earthquake, and E_s/M_0. Shapiro *et al.* (1998) and Iglesias (*et al.*, 2003) computed E_r from the relation:

$$E_s = \frac{\int_0^5 V^2(f)df}{\int_1^5 V^2(f)df}, \qquad (2)$$

where $V^2(f) = V_N^2(f) + V_E^2(f) + V_Z^2(f)$, and $V_i(f)$ is the Fourier spectrum of the i-th component of the velocity recorded at CUIG, normalized to a distance of 400 km. For normalization, geometrical spreading was assumed to be as R^{-1} for R<100 km (body waves) and as $R^{-1/2}$ (surface waves) beyond 100 km. The quality factor, Q, was taken as $Q(f)=273f^{0.67}$ (Ordaz and Singh, 1992). Fig. 3 illustrates E_r versus M_w plot for 21 earthquakes. It includes two earthquakes from Peru (events 18 and 19). Event 18 (21 February, 1996; M_w=7.5, M_s=6.6; m_b=5.8) was a "tsunami" earthquake (as also indicated by a large disparity between M_w and M_S). This event has the largest E_r value in the figure. On the other hand, E_r of event 19 (12 November, 1996) is small. Aftershocks locations suggest that events 18 and 19 occurred near the trench and near the coast, respectively (Shapiro *et al.*, 1998). Dashed curve in Fig. 3 illustrates E_r versus M_w curve for ω^2 source model of Brune (1970) at a distance of 400 km. In computing the theoretical curve, we have taken the same $Q(f)$ and the geometrical spreading as used in the normalization of the data. A constant stress drop of 2 MPa has been taken in the calculation. With two exceptions, the events above the dashed curve in Fig. 3 occurred offshore while those that fall below it were located near the coast. The figure suggests that farther above the E_r value of an earthquake with respect to the reference ω^2 curve, the higher is its tsunami potential. Since such an earthquake is deficient in high-frequency radiation, it is expected to produce smaller acceleration. Conversely, lower the E_r value with respect to the reference curve, smaller is the tsunami potential but higher is the expected acceleration.

The National Seismological Service (SSN) of Mexico reports magnitudes of moderate and large earthquakes based on broadband seismograms recorded at CUIG (Singh and Pacheco, 1994). This algorithm may be modified to compute both the magnitude and E_r in near-real time.

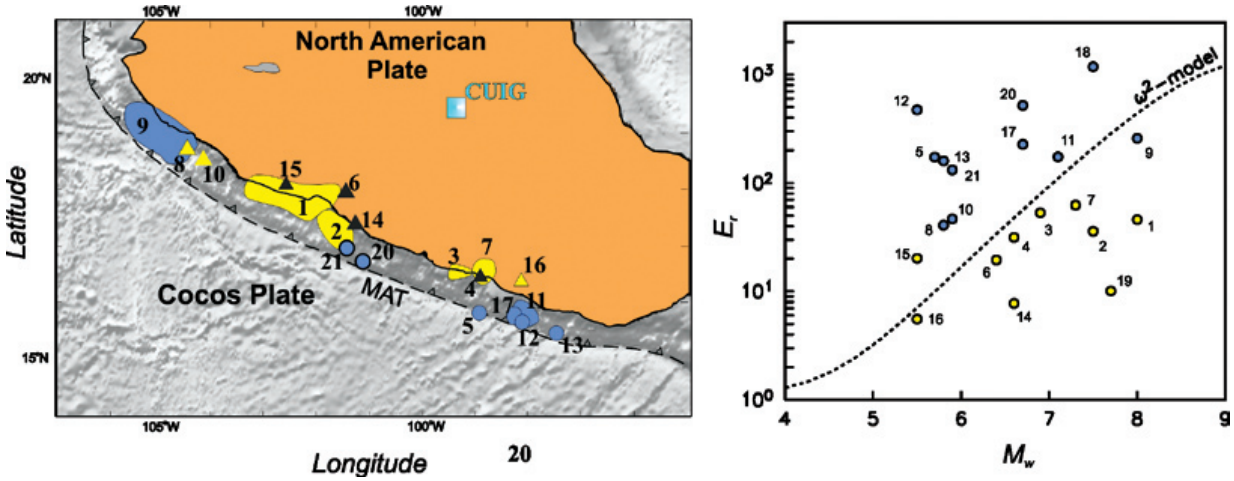

Fig. 3. (Left) Location of earthquakes along the Mexican subduction zone whose E_r values have been computed. (Right) E_r versus M_w (modified from Iglesias, *et al.*, 2003). Event 9 corresponds to Colima-Jalisco earthquake of 1995 (M_w=8.0). Events 18 (21 February, 1996; M_w=7.5) and 19 (12 November, 1996; M_w=7.7) are from the Peruvian coast. Event 18 was a "tsunami" earthquake.

Two examples:
1. The Colima-Jalisco earthquake of 1995

The coseismic static displacement caused by this earthquake was obtained from campaign-mode GPS measurements carried out before and after the earthquake (Melbourne *et al*., 1997). The data, shown in Fig. 4, provide a test for the estimation of the seismic moment, the location and the size of the rupture area. We note that the vertical displacement, U_z, was negative along the coast. The tide gauge record at Manzanillo also shows a subsidence (Ortiz *et al*., 2000). The subsidence of the coast implies that the rupture extended less than ~13 km inland from the coast. The horizontal displacement rapidly decreases between stations CHAM and CHAC to the NW and between CRIP and SJDL to the SE. This suggests that the fault extended from ~50 km NW of CHAM to ~50 km SE of CRIP, for a total rupture length, L, of ~180 km. As mentioned earlier, the width, W, of the coupled interface along the Mexican subduction zone that ruptures in great earthquakes is about 80 km. These estimates are in excellent agreement with those obtained from a detailed aftershock study by Pacheco *et al*. (1997): rupture reaching up to the coast, L=170 km, and W=70 km. The average of horizontal displacement at CHAM and CRIP is 75 cm. This observation, along with L=180 km and W=80 km, requires an average dislocation of 2.5 m on the fault. This yields a seismic moment, $M_0 = \mu LWD$, of 1.3×10^{21} Nm (M_w=8.0), surprisingly close to $M_0=1.15 \times 10^{21}$ Nm (M_w=8.0) reported in Harvard CMT catalog. This case demonstrates that closely-spaced, continuously-operating GPS stations along the Mexican coast, with the capacity to track the positions of the stations in near real time, would be very useful in quick estimation of the seismic moment, and the location and size of the rupture area of $M_w \geq 8.0$ earthquakes.

As mentioned above, a rapid estimation of the radiated energy, E_s, can provide a clue to the tsunami potential or the damage potential due to intense ground motion. For the Colima-Jalisco earthquake of 1995 we follow the step outlined above. We use the aftershock of 12 October, 1995 (M_w=5.9) as the EGF. Fig. 5 shows the moment rate function $\dot{M}_0(f)$ of the target event. The figure also gives theoretical $\dot{M}_0(f)$ for ω^2-source model with a stress drop of 4 MPa. We estimate E_s at frequencies $f \leq 0.2$ Hz from $\dot{M}_0(f)$ shown in the figure using equation (1a). The contribution to E_s of frequencies $f > 0.2$ Hz is obtained assuming ω^{-2} fall off of $\dot{M}_0(f)$ above 0.2 Hz (green line), using equation (1c), with $\dot{M}_0(f_u) = 2.88 \times 10^{19}$ Nm at f_u=0.2 Hz (Fig. 5). The total E_s is 8.84×10^{15} J. This gives $E_s/M_0 = 7.7 \times 10^{-6}$, a slightly lower that normal value for large/great subduction zone earthquakes (Venkataraman and Kanamori, 2004; Weinstein and Okal, 2005). For comparison, Venkataraman and Kanamori (2004) report E_s of 4-8x10^{15} J from telesesimic P waves. This suggests that a rapid and reliable estimation of E_s of great Mexican earthquakes is possible using the EGF technique provided that a library of properly cataloged seismograms of earthquakes of $M_w \leq 6.0$ are available in the computer memory for immediate retrieval. Since the upper limit of integration, f_u, in equation (1) is critical; its value should be known for each EGF event in advance.

The ratio of total- to high-frequency energy, E_r, for the Colima-Jalisco earthquake was 258 (event 9, Fig. 3, a value slightly below the reference curve corresponding to the ω^2-source model. For comparison, E_r for the 1985 Michoacan earthquake was 46 (event 1, Fig. 3). While E_r of the 1995 earthquake does not suggest a "tsunami" earthquake, it does point towards a more tsunamigenic earthquake than the 1985 earthquake. This, indeed, was the case as documented by inundation heights (M. Ortiz, personal communication, 2008).

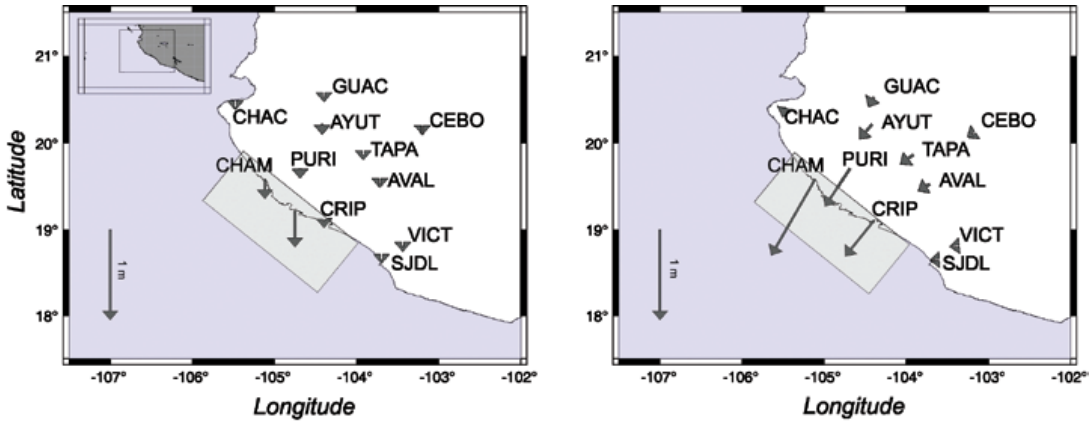

Fig. 4. Coseismic static displacement for the Colima-Jalisco earthquake of 9 October, 1995 (modified from Melbourne *et al*., 1997). (Left) Vertical component. (Right). Horizontal component. The location and the size of the rectangular area is a rough approximation of the rupture area. It is based on the static displacement shown in the figure (see text).

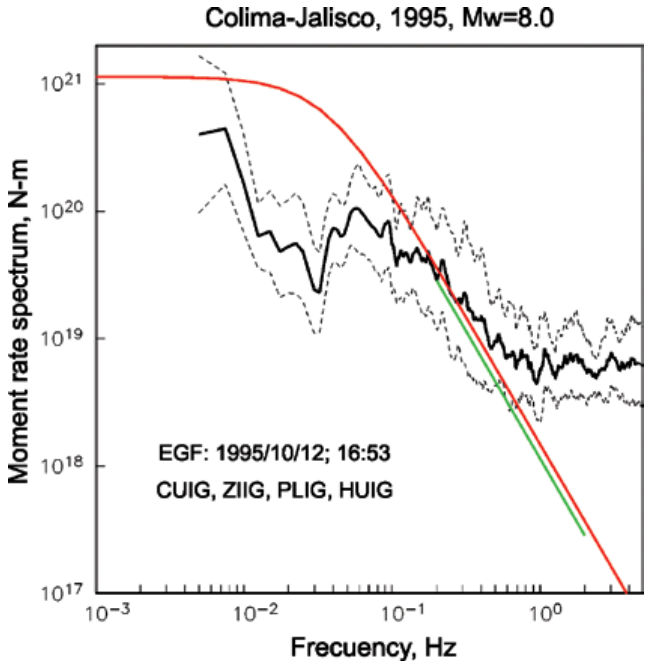

Fig. 5. Colima-Jalisco earthquake of 1995 (black continuous curve), using the EGF technique. The red line corresponds to a theoretical ω^2-source model with M_0=1.15x10^{21} Nm and stress drop ($\Delta\sigma$) of 4 MPa. Equation 1 was used to estimate E_s for f≤0.2 Hz. Contribution of f>0.2 Hz to E_s was computed assuming ω^{-2} fall off of $\dot{M}_0$ (f)above 0.2 Hz (green line).

Thus, a coherent picture of the Colima-Jalisco earthquake emerges from GPS displacement vectors, and estimates of E_s and E_r: the rupture was essentially offshore of L~180 km and W probably 80 km, M_0=1.3x10^{21} Nm (M_w=8.0), E_s/M_0=7.7x10^{-6}, and E_r=258. Off-shore rupture, and relatively low value of E_s/M_0 and high value of E_r suggest an earthquake with somewhat high tsunamigenic potential. It is noteworthy that these parameters are very similar to those obtained from detailed analyses. This gives us confidence that rapid and reliable estimation of these parameters for great Mexican earthquakes may be possible if, in addition to the broadband seismographic network, a dense GPS network becomes operational along the coast so that the positions of the stations can be tracked in near real time.

2. The Sumatra-Andaman earthquake of 2004

Finally, we test whether rapid and automatic analysis of near-field static displacements could have yielded a reliable seismic moment of the giant Sumatra-Andaman earthquake (26 December, 2004), had the data been available in near-real time. We also test whether the EGF technique would have provided reasonable estimate of the radiated energy, E_s.

We note that the near-field static displacements for the 2004 earthquake were obtained from GPS measurements carried out before and after the earthquake, in a campaign mode. Near- and far- field geodetic data have been analyzed by themselves (e.g., Vigny *et al*., 2006; Banerjee *et al*., 2005, 2007; Gahalaut *et al*., 2006; Rajendran *et al*., 2007) as well as in conjunction with the seismic data (e.g., Chlieh *et al*., 2007) to invert for the slip distribution on the fault. As expected, the slip distribution is complex. For our test, we selected the near-field static deformation reported in Gahalaut *et al*. (2006). These values have not been corrected for post-seismic slip, which was small (Banerjee *et al*., 2007; V. Gahaluat, personal communication, 2008). Fig. 6 shows the horizontal coseismic displacement on the surface. Note that the near-field data are available only between 7° and 14° N. The average amplitude of the horizontal vectors in Fig. 6 is 4.1 m. Since the epicenter was located near 3°N, we assume that the average displacement was the same above the fault segment between 2° and 7°N (the inversion of seismic and geodetic data, in fact, yield larger displacement above this segment). Although the rupture propagated along an arc, we approximate the fault by a rectangle of length, L, of 1330 km (from 2° to 14° N). We take the dip of the fault, δ, as 15°, the width W as 150 km, and the depth of the deep edge of the fault as 50 km. These parameters are supported by seismicity of the region (e.g., Engdahl *et al*., 2007). Finally, we assume that

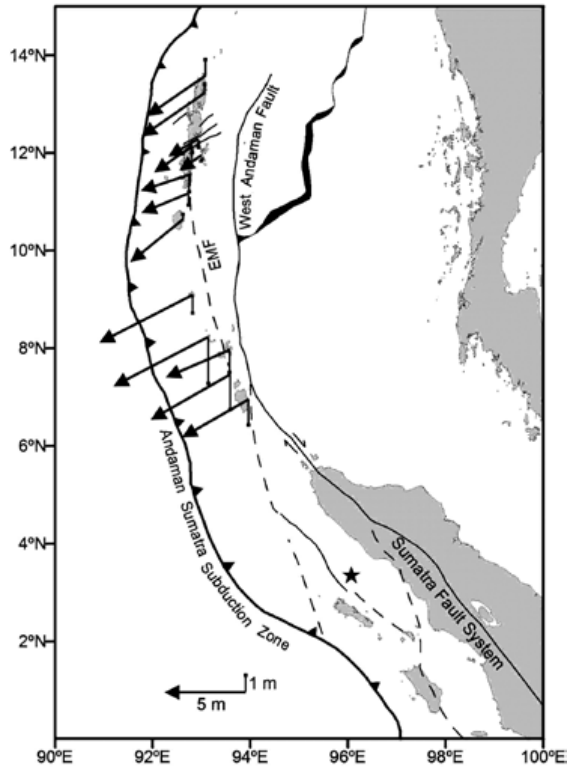

Fig. 6. Horizontal near-field static displacement vectors (black arrows) caused by the Sumatra-Andaman earthquake of 26 December 2004. The data were obtained from campaign mode observations (from Gahalaut *et al*., 2006). The vectors are not corrected for post-seismic creep which is expected to be small. (V. Gahalaut, personal communication, 2008; Banerjee *et al*., 2007). The average horizontal displacement is 410 cm.

the static displacements were measured at points above the deep edge of the fault (along a line defined by z=0, y=0 in Fig. 2). This is incorrect since the field observations and the geodetic data from GPS campaign demonstrate that some islands in the Andaman and Nicobar region were uplifted, while others suffered subsidence. However, as Fig. 2 shows, the horizontal displacement is not very sensitive to the exact location of the observation point with respect to the rectangular fault area below. Under these reasonable assumptions, an average dislocation, D, of 12 m is needed to produce a horizontal displacement of 4.2 m at the surface. Assuming μ=6x10^4 MPa, this yields a seismic moment $M_0=\mu LWD$ of 1.17x10^{23} Nm (M_w=9.3). The magnitude of the Sumatra-Andaman earthquake has been controversial; the estimates, using different data sets and techniques, vary between M_w=9.0 and 9.3 (see Bilek *et al*., 2007 for a summary). Our estimate is in the range of the values reported in studies based on detailed analysis of the data. We reiterate that this estimate could have been obtained within about 20 minutes after the earthquake, had the positions of GPS stations in the near field been available in near real time.

We estimated E_s of the 2004 earthquakes using an aftershock which occurred on 2 January, 2005 (6.25°N, 92.47°E, Mw=6.3) as the EGF. The depth of the EGF is given as 12 km in Harvard CMT catalog and 25 km in Engdahl *et al*. (2007). Fig. 7 (top) shows $\dot{M}_0(f)$ of the Sumatra earthquake retrieved from the EGF technique (continuous black curve). The figure includes $\dot{M}_0(f)$ reported by Stein and Okal (2005) at ultra-low frequencies and in Global Centroid Moment-Tensor (GCMT) catalog (http://www.globalcmt.org/CMTsearch.html) at about 0.0025 Hz. Also included in the figure is the $\dot{M}_0(f)$ corresponding to the source time function of model III of Ammon *et al*. (2005). We note that $\dot{M}_0(f)$ from the EGF technique and from model III are fairly consistent in the frequency range of 0.005-0.1 Hz. We computed E_s in this frequency band using equation (1a), assuming ρ=3.2 gm/cm^3 and β=4.62 km/s. The result is shown in Fig. 7 (bottom) as a function of azimuth. For the entire data set, log E_s=16.97±0.30 which gives a median E_s=9.29x10^{16} J. E_s in the frequency band 0-0.005 Hz is 7.0x10^{15} J. Median $\dot{M}_0(f_u)$ at f_u=0.1 Hz is 1.72x10^{20} Nm (Fig. 7). This yields E_s=1.11x10^{16} J for f >0.1 Hz (equation 1c). Thus, our estimate of total E_s is

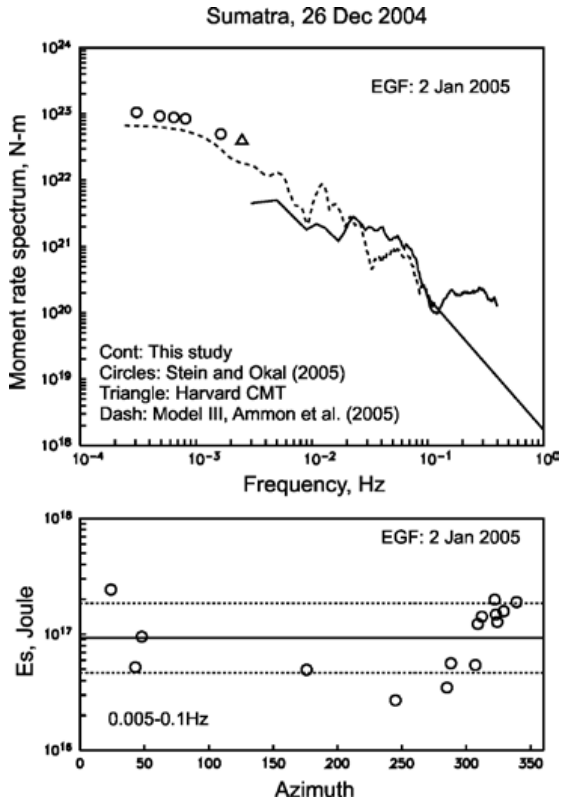

Fig. 7. (Top) $\dot{M}_0(f)$ Sumatra-Andaman earthquake of 2004 (black continuous curve), using the EGF technique, obtained in this study. Equation (1a) was used to estimate E_s for $f \leq 0.1$ Hz. Contribution of $f > 0.1$ Hz to E_s was computed assuming ω^{-2} fall off and triangle above 0.1 Hz (green line). Circles denote $\dot{M}_0(f)$ obtained by Stein and Okal (2005) from free-oscillation data. Triangle: moment reported in Harvard CMT catalog. Dashed line represents $\dot{M}_0(f)$ corresponding to the source time function of model III of Ammon *et al*. (2005). (Bottom) E_s as function of azimuth in the frequency band 0.005-0.1 Hz.

1.11×10^{17} J. For comparison, Choy and Boatwright (2007) and Kanamori (2006) report $E_s = 1.4 \times 10^{17}$ J and 3.0×10^{17} J, respectively. These values are unexpectedly close to the one reported here. Our estimate of radiated energy differs from that by Kanamori (2006) mostly at frequencies higher than 0.1 Hz: 1.11×10^{16} J versus 1.6×10^{17} J.

From $E_s = 1.11 \times 10^{17}$ J and $M_0 = 1.2 \times 10^{23}$ Nm estimated here, $E_s/M_0 = 1.1 \times 10^{-6}$. If we consider the range of the reported values of E_s ($1.1\text{-}3.0 \times 10^{17}$ J) and M_0 ($0.6\text{-}1.3 \times 10^{23}$ Nm), then Es/M_0 ranges between 1.1×10^{-6} and 5.0×10^{-6}, values smaller than that of other large/great subduction zone earthquakes.

Some further considerations and future work

This exploratory study is based on some assumptions and expectations that deserve further validation and checking. For example, in our discussion of GPS data we have assumed a uniform slip on the fault. The slip during a large/great earthquake will be heterogeneous. The assumption of uniform slip is expected to have relatively small effect on the estimation of the seismic moment and the length of the rupture (provided that the coast GPS coverage is adequate). However, the location of the rupture area, estimated from the sense of the vertical motion, may be more sensitive to this assumption. Clearly, a more exhaustive testing is warranted.

The permanent GPS network of the Instituto de Geofísica, UNAM, presently includes 13 autonomous stations along the coast with an average separation of ~200 km (Fig. 8). If rapid information is required for only $M_w \geq 8.0$ earthquakes (length of rupture greater than ~130 km), then the station separation along the coast should be ~65 km. Since the coast from Puerto Vallarta to Tapachula is ~1600 km long, the total number of GPS stations should be 28; thus 15 additional stations along the coast will be needed. This would be the minimum number of stations required. However, more redundancy in the system would be highly desirable. The system may be complimented with data from inland GPS stations. It

will be advantageous to install tiltmeters along the coast and add these stations to the network. Some limitations of tiltmeters is discussed by Lomnitz (1997). Real-time transmission of the data from the stations to a central location and tracking of the position of the stations in near-real time will be crucial. We are not the first to suggest supplementing broadband seismograms with tracking of GPS station positions to estimate magnitudes for tsunami warning (see, e.g., Blewitt *et al*., 2006). A GPS shield has recently been proposed for early tsunami warning in Sumatra (Sobolev *et al*., 2007).

We have proposed the use of the empirical Green's function (EGF) technique to compute the radiated energy, E_s. To a great extent, the success of the EGF method depends on an appropriate selection of the EGF event. A library of seismograms for earthquakes of $M_w \leq 6.0$, which sample the entire Pacific coast of Mexico, should be saved in computer memory so that they may be retrieved quickly. The source parameters of the EGF events (location, depth, seismic moment, focal mechanism, corner frequency) would have to be carefully determined beforehand. As near-source broadband seismograms are likely to saturate during great earthquakes, the recordings of EGF events should also be available at large distances (R>500 km). In view of the fact that a scarcity of M~6 earthquakes has previously been reported for the Mexican subduction zone (Singh *et al*., 1983), a critical issue is whether recordings of adequate EGFs are presently available. We searched the GCMT catalog beginning 1995 for shallow, thrust earthquakes along the Mexican coast with Mw≤6.2. The events are plotted in Fig. 9. These earthquakes have been recorded by the Mexican broadband seismographic network. The figure shows some large gaps along the coast and suggests that smaller-magnitude earthquakes would have to be used as EGFs in some segments of the subduction zone. Although recordings of such events exist, we need to carefully assess the suitability these events as appropriate EGFs and estimate their relevant source parameters. Generally, the use of different EGFs yields estimates of E_s which only differ by a factor of about two (e.g., Venkataraman *et al*., 2002; Singh *et al*., 2004). Thus, all EGFs which fall in the estimated rupture area of the mainshock can be used in the calculation of E_s without requiring further selection criterion.

Concluding Remarks

We have shown that a rapid and reliable estimation of the moment magnitude (M_w), the location and the size of the rupture area, the radiated energy (E_s), and the ratio of total- to high-frequency energy (E_r) is viable for great earthquakes ($M_w \geq 8.0$) along the Mexican subduction zone, provided that regional BB seismograms and

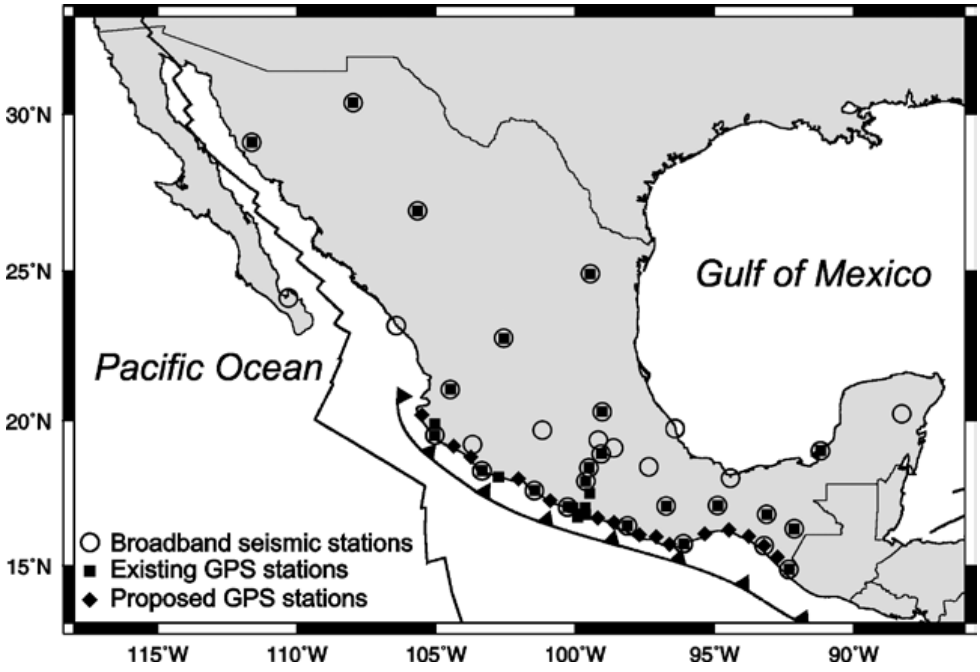

Fig. 8. Broadband seismological network (circles) and GPS network (rectangles) of Instituto de Geofisica, UNAM. Proposed GPS stations are shown by diamonds. The present and proposed GPS network will ensure at least two stations in the epicentral region of great coastal earthquakes ($M_w \geq 8.0$). However, for redundancy a larger number of stations will be highly desirable.

continuous GPS position are available in near-real time. This information can be obtained within about 15-20 minutes after the occurrence of an earthquake: it would be very helpful for a quick assessment of tsunami occurrence and/or damage potential of the event, and in issuing an early tsunami alert. The peak tsunami wave occurs at the near-source coast of Mexico 10 to 20 minutes after the earthquake. Thus an early alert, based on the estimation of the source parameters mentioned above, is not possible for the coastal area close to the source. However, it may be useful in adjacent areas. If, however, an early alert is to be based only on M_w, then this may be accomplished in less than 6-7 minutes from the analysis of the GPS data. It is worth noting that an estimate of M_w may also be possible in short time (about 6-7 minutes) from the analysis of W-phase recorded on the regional broadband seismographs (H. Kanamori, personal communication, 2008). W-phase is a long-period wave that is predicted from theory to arrive between P and S phases. It is observed on broadband seismograms (see, e.g., Kanamori and Kikuchi, 1993).

A rapid estimation of the critical source parameters will complement some other initiatives of near-real-time seismology in Mexico. These initiatives are: (1) the seismic alert system (SAS) for Mexico City, in operation since 1992. (2) Rapid estimation of ground motion parameters in Mexico City, in a first stage of development at the Instituto de Ingenieria (II), UNAM. (3) Contours of observed ground-motion in Mexico, presently under development at II, UNAM. The alert and the ground-motion maps can only be understood in proper perspective if the critical source parameters of the earthquake are known.

A high-sampling, preferably 1 Hz, GPS is an ideal strong-motion seismograph which records displacement. Thus, an improved and enlarged 1 Hz GPS network, along with the existing broadband seismographic and accelerographic networks of Mexico, will provide valuable data for inversion of spatio-temporal evolution of rupture on the fault plane. The GPS data is critical in the study of earthquake cycle, interplate coupling, seismotectonics, and geodynamics. Observations based on GPS in Mexico (e.g., Kostoglodov *et al*., 2003; Iglesias *et al*., 2004; Larson *et al*., 2007) and elsewhere have led to the discovery of silent earthquakes on the plate interface. An enlarged network may answer some of the critical questions which remain unanswered, e.g., the precise location of the area below Mexico that slips during a silent earthquakes.

Acknowledgments

We thank V. Gahalaut for helpful discussions and for providing us with Fig. 6. Incisive comments and suggestions by Gregory Beroza and an anonymous reviewer are greatly appreciated. The research was partially funded by DGAPA, UNAM project IN114307 and IN11027 and FOPREDEN-GDF.

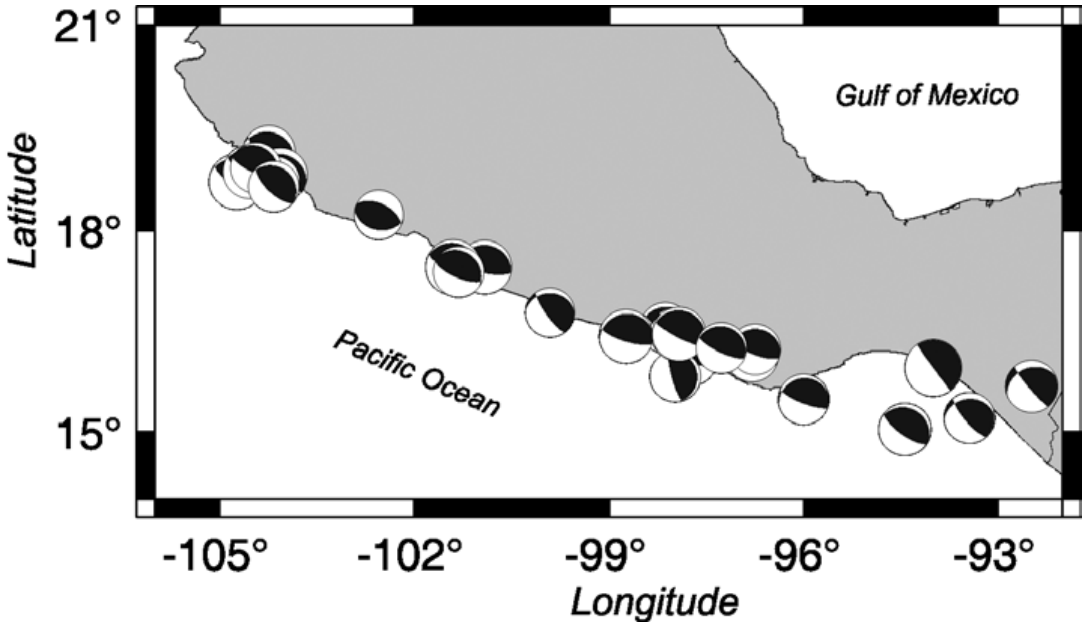

Fig. 9. Shallow, thrust earthquakes ($M_w \leq 6.2$) along the Mexican subduction zone since 1995 listed in the Global Centroid Moment Tensor catalog whose regional broadband recordings are available and can be used be as empirical Green's functions (EGFs) to estimate radiated seismic energy of large/great earthquakes. As these earthquakes do not adequately cover the entire subduction zone, recorded seismograms of smaller-magnitude earthquakes may also have to be used as EGFs in some segments.

Bibliography

Ammon, C. J., H. Kanamori, T. Lay and A. A. Velasco, 2006. The 17 July 2006 Java tsunami earthquake, *Geophys. Res. Lett., 33*, L24308, doi:10.1029/2006GRL028005.

Ammon, C. J., C. Ji, H. -T. Thio, D. Robinson, S. Ni, V. Hjorleifsdottir, H. Kanamori, T. Lay, S. Das, D. Helmberger, G. Ichinose, J. Polet and D. Wald, 2005. Rupture process of the 2004 Sumatra-Andaman earthquake, *Science, 308*, 1133-1139.

Anderson, J. G., P. Bodin, J. Brune, J. Prince, S. K. Singh, R. Quass and M Oñate 1986. Strong ground motion from the Michoacan, Mexico earthquake, *Science, 233*, 1043-1049, 1986.

Banerjee, P., F. F. Pollitz and R. Bürgmann, 2005. The size and duration of the Sumatra-Andaman earthquake from far-field static offsets, *Science, 308*, 1769-1772.

Banerjee, P., F. F. Pollitz, B. Nagarajan and R. Bürgmann 2007. Coseismic slip distributions of the 26 December Sumatra-Andaman and 28 March 2005 Nias earthquakes from GPS static offsets, *Bull. Seism. Soc. Am., 97*, S86-S102.

Bilek, S. L., K. Satake and K. Sieh, 2007. Introduction to the special issue on the 2004 Sumatra-Andaman earthquake and the Indian ocean tsunami, *Bull. Seism. Soc. Am., 97*, S1-S5.

Blewitt, G., C. Kreemer, W. C. Hammond, H. -P. Plag, S. Stein and E. Okal, 2006. Rapid determination of earthquake magnitude using GPS for tsunami warning systems, *Geophys. Res. Lett., 33*, L11309, doi: 10.1029/2006GL026145.

Boatwright, J. and G. L. Choy, 1986. Teleseismic estimates of the energy radiated by shallow earthquakes, *J. Geophys. Res., 91*, 2095-2112.

Bodin, P. and T. Klinger, 1986. Coastal uplift and mortality of intertidal organisms caused by the September 1985 Mexico earthquakes, *Science, 233*, 1071-1073.

Boore, D., 2001. Effect of baseline corrections on displacements response spectra for several recordings of the 1999 Chi-Chi, Taiwan, earthquake, *Bull. Seism. Soc. Am., 91*, 1199 –1211.

Brune, J. N., 1970. Tectonic stress and spectra of seismic shear waves from earthquakes, *J. Geophys. Res., 75*, 4997-5009, 1970. (Correction, *J. Geophys. Res., 76*, 5002, 1971.)

Clinton, J. F., 2004. Modern digital seismology—instrumentation, and small amplitude studies in the engineering world, Ph.D. Thesis, California Institute of Technology.

Chael, E. and G. S. Stewart, 1981. Recent large earthquakes along the middle America trench and their tectonic implications for the subduction process, *J. Geophys. Res., 103*, 329-338.

Chlieh, M. *et al*., 2007. Coseismic slip and afterslip of the great Mw 9.15 Sumatra-Andaman earthquake of 2004, *Bull. Seism. Soc. Am., 97*, S152-S173.

Choy, G. L. and J. Boatwright, 2007. The energy radiated by the 26 December 2004 Sumatra-Andaman earhtquke estimated from 10-minute P-wave windows, *Bull. Seism. Soc. Am., 97*, S18-S24.

Emore, G. L., J. S. Haase, K. Choi, K. M. Larson and A. Yamagiwa, 2007. Recovering seismic displacements through combined use of 1-Hz GPS and strong-motion accelerometers, *Bull. Seism. Soc. Am., 97*, 357-378.

Engdahl, E. R., A. Villaseñor, H. R. Deshon and C.h. Thurber, 2007. Teleseismic relocation and assessment of seismicity (1918-2005) in the region of the 2004 Mw9.0 Sumatra-Andaman and 2005 Mw8.6 Nias Island great earthquakes, *Bull. Seism. Soc. Am., 97*, S43-S61.

Farreras, S. F., 1997. Tsunamis en México. En: Oceanografía Física en México (editor: M.F. Lavin), Monograma No. 5, Unión Geofísica Mexicana.

Gahalaut, V., B. Nagarajan, J. K. Catherine and S. Kumar, 2006. Constraint on 2004 Sumatra-Andaman earthquake rupture from GPS measurements in Andaman-Nicobar Islands, *Earth Planet. Sci. Lett., 242*, 365-374.

Iglesias, A., S. K. Singh, J. F. Pacheco, L. Alcántara, M. Ortiz and M. Ordaz, 2003. Near trench Mexican earthquakes have anomalously low peak accelerations, *Bull. Seism. Soc. Am., 93*, 953-959.

Iglesias, A. and S. K. Singh, 2007. Estimation of radiated energy using the EGF technique: what should be the upper limit of integration in the frequency domain? *Bull. Seism. Soc. Am., 97*, 1346- 1349.

Iglesias, A., S. K. Singh, A. R. Lowry, M. Santoyo, V. Kostoglodov, K. M. Larson and S. I. FrancoSsánchez, 2004. The silent earthquake of 2002 in the Guerrero seismic gap, Mexico (M_w=7.6): Inversion of slip on the plate interface and some implications, *Geofísica Internacional, 43*, 309-317.

Iwan, W. D., M. A. Moser and C. -Y. Peng, 1985. Some observations on strong-motion earthquake measurement using a digital accelerograph, *Bull. Seism. Soc. Am., 75*, 1225- 1246.

Kanamori, H., 1972. Mechanisms of tsunami earthquakes, *Phys. Earth Planet. Interiors, 6*, 346 –359.

Kanamori, H., 2006. The radiated energy of the 2004 Sumatra-Andaman earthquake, in Earthquakes: radiated energy and the physics of faulting, edited by R. Abercrombie, A. McGarr, H. Kanamori, and G. Di Toro. Geophysical Monograph Series 170, American Geophysical Union, Washington, D.C., 59-68.

Kanamori, H. and M. Kikuchi, 1993. The 1992 Nicaragua earthquake: a slow tsunami earthquake associated with subducted sediments, *Nature, 361*, 714-716.

Kostoglodov, V., S. K. Singh, J. A. Santiago, S. I. Franco, K. M. Larson, A. R. Lowry and R. Bilham, 2003. A large silent earthquake in the Guerrero seismic gap, Mexico, *Geophys. Res. Lett., 30*, 1807, doi:10.1029/2003GL017219.

Larson, K. M., V. Kostoglodov, S. Miyazaki and J. A. Santiago, 2007. 2006 aseismic slow slip event in Guerrero, Mexico: new results from GPS, *Geophys. Res. Lett., 34*, L13309, doi:1029/2007GL029912.

Lay, T., H. Kanamori, C. J. Ammon, M. Nettles, S. N. Ward, R. C. Aster, S. L. Beck, S. L. Bilek, M. R. Brudzinski, R. Buttler, H. R. Deshon, G. Ekström, K. Satake and S. Sipkin, 2005. The great Sumatra-Andaman earthquake of 26 December 2004, *Science, 308*, 1127-1133.

Lomnitz, C., 1997. Frequency response of a strainmeter, *Bull. Seism. Soc. Am., 87*, 1078-1080.

Melbourne, T., I. Carmichael, C. DeMets, K. Hudnut, O. Sanchez, J. Stock, G. Suarez and F. Webb, 1997. The geodetic signature of the M8.0 October 9, 1995, Colima-Jalisco, Mexico, *Geophys. Res. Lett., 24*, 715-718.

Newman, A. V. and E. A. Okal, 1998. Teleseismic estimates of radiated seismic energy: the E/M_0 discriminant for tsunami earthquakes, *J. Geophys. Res., 103*, 26,885 –26,898.

Núñez-Cornu, F. J., M. Ortiz and J. J. Sánchez Aguilar, 2008. The great 1787 Mexican tsunami, *Nat. Hazards*, doi:10.1007/s11069-008-9239-1.

Okada, Y., 1992. Internal deformation due to shear and tensile faults in a half space, *Bull. Seism. Soc. Am., 82*, 1018-1040.

Ordaz, M. and S. K. Singh, 1992. Source spectra and spectral attenuation of seismic waves from Mexican earthquakes, and evidence of amplification in the hill zone of Mexico City, *Bull. Seismol. Soc. Am., 82*, 24-43.

Ortiz, M., V. Kostoglodov, S. K. Singh and J. F. Pacheco, 2000. New constraints on the uplift of October 9, 1995 Jalisco-Colima earthquake (M_w=8) based on the analysis of tsunami records at Manzanillo and Navidad, Mexico, *Geofísica Internacional, 39*, 349-357.

Pacheco, J. F. , S. K. Singh, J. Dominguez, A. Hurtado, L. Quintanar, Z. Jimenez, J. Yamamoto, C. Gutierrez, M, Santoyo, W. Bandy, M. Guzman and V. Kostoglodov, 1997. The October 9, 1995 Colima-Jalisco, Mexico, earthquake (M_w 8): An aftershock study and a comparison of this earthquake with those of 1932. *Geophys. Res. Lett., 24*, 2223-2226.

Pacheco, J. F. and S. K. Singh, 2008. Seismicity and the state of stress along the Guerrero, Mexico, subduction zone, in preparation.

Park, J., T-R. Alex Song, J. Tromp, E. Okal, S. Stein, G. Roult, E. Clevede, G. Laske, H. Kanamori, P. Davis, J. Berger, C. Braitenberg, M. Van Camp, X. Lei, H. Sun, H. Xu and S. Rosat, 2005. Earth's free oscillations excited by the 26 December 2004 Sumatra-Andaman Earthquake, *Science, 308*, 1139-1144.

Pérez-Campos, X., S. K. Singh and G. Beroza, 2003. Reconciling teleseismic and regional estimates of seismic energy, *Bull. Seism. Soc. Am., 93*, 2123-2130, 2003.

Rajendran, C. P., K. Rajendran, R. Anu, A. Earnest, T. Machado, P. M. Mohan and J. Freymueller, 2007. Crystal deformation and seismic history associated with the 2004 Indian Ocean earthquake: a perspective from Andaman-Nicobar Islands, *Bull. Seism. Soc. Am., 97*, S174-S191.

Shapiro, N. M., S. K. Singh and J. F. Pacheco, 1998. A fast and simple diagnostic method for identifying tsunamigenic earthquakes, *Geophys. Res. Lett. 25,* 3911 –3914.

Singh, S. K., M. Rodriguez and L. Esteva, 1983. Statistics of small earthquakes and frequency of occurrence of large earthquakes along the Mexican subduction zone, *Bull. Seism. Soc. Am., 73*, 1779-1796.

Singh, S. K., G. Suárez and T. Domínguez, 1985. The Oaxaca, Mexico earthquake of 1931: lithospheric normal faulting in the subducted Cocos plate, *Nature, 317*, 56-58.

Singh, S. K. and F. Mortera, 1991. Source-time functions of large Mexican subduction earthquakes, morphology of the Benioff age of the plate and their tectonic implication, *J. Geophys. Res., 96*, 21487-21502.

Singh, S. K. and J. F. Pacheco, 1994. Magnitude of Mexican earthquakes, *Geofisica Internacional, 33*, 189-198.

Singh, S. K. and M. Ordaz, 1994. Seismic energy release in Mexican subduction zone earthquakes, *Bull. Seism. Soc. Am., 84*, 1533-1550.

Singh, S. K., J. F. Pacheco, B. K. Bansal, X. Pérez-Campos, S. N. Bhattacharya, R. S. Dattatrayam and G. Suresh, 2004. A source study of Bhuj, India, earthquake of 26 January, 2001 (Mw=7.6), *Bull. Seism. Soc. Am., 94*, 1195-1206.

Sobolev, S. V., et al., 2007. Tsunami early warning using GPS-Shield array, *J. Geophys. Res., 112*, B08415, doi: 10.1029/206JB004640.

Stein, S. and E. Okal, 2005. Speed and size of the Sumatra earthquake, *Nature, 434*, 581-582.

Suárez, G., T. Monfret, G. Wittlinger and C. David, 1990. Geometry of subduction zone and depth of the seismogenic zone in the Guerrero gap, Mexico, *Nature, 345*, 336-338.

Suárez, G. and P. Albini, 2008. Evidence for Great Tsunamigenic Earthquakes (M8.6) along the Mexican Subduction Zone *Bull. Seismol. Am.* in press

UNAM Seismology Group, 1986. The September 1985 Michoacan earthquakes: Aftershock distribution and history of rupture, *Geophys. Res. Lett., 13*, 573-576.

Vassiliou, M. S. and H. Kanamori, 1982. The energy release in earthquakes, *Bull. Seism. Soc. Am., 72*, 371-387.

Venkataraman, A., L. Rivera and H. Kanamori, 2002. Radiated energy from the 16 October 1999 Hector Mine earthquake: regional and teleseismic estimates, *Bull. Seism. Soc. Am., 92*, 1256-1265.

Venkataraman, A. and H. Kanamori, 2004. Observational constraints on the fracture energy of subduction zone earthquakes, *J. Geophys. Res., 109*, B05302, doi: 10.1029/2003JB002549.

Vigny, C., et al., 2005. Insight into the 2004 Sumatra-Andaman earthquake from GPS measurements in Southeast Asia, *Nature, 436*, 201-206.

Weinstein, S. A. and E. Okal, 2005. The mantle magnitude M_m and the slowness parameter Θ: five years of real-time use in the context of tsunami warning, *Bull. Seism. Soc. Am., 85*, 779-799.

S. K. Singh[1*], X. Pérez-Campos[1], A. Iglesias[1] and J. F. Pacheco[1]

[1]Instituto de Geofísica, Universidad Nacional Autónoma de México, Del. Coyoacán, 04510 Mexico City, Mexico

**Corresponding author: krishna@geofisica.unam.mx*